Time-resolved resonance Raman spectroscopy and density functional theory investigation of the CH$_2$I–I isomer and CH$_2$I$_2$···I molecular complex products produced from ultraviolet photolysis of CH$_2$I$_2$ in the solution phase: Comparison of the structure and chemical reactivity of polyhalomethane isomers and polyhalomethane–halogen atom molecular complexes

Yun-Liang Li, Dongqi Wang, and David Lee Phillips[a]
Department of Chemistry, University of Hong Kong, Hong Kong

Time-resolved resonance Raman spectra are reported for different concentrations of CH$_2$I$_2$ in cyclohexane solution. The CH$_2$I–I species is observed at low concentrations and it decays on the order of tens of nanoseconds to almost no signal at 100 ns and no other signal is observed up to 15 microseconds. Two species are observed at high concentrations. The first species CH$_2$I–I spectra and lifetime are about the same as that found at low concentration of CH$_2$I$_2$ parent molecule and the second species is a CH$_2$I$_2$···I molecular complex observed on the nanosecond to microsecond time scale and formed from bimolecular reaction of iodine atoms with CH$_2$I$_2$ molecules. The chemical reactivity of the CH$_2$I–I species and the CH$_2$I$_2$···I molecular complex towards carbon double bonds were investigated using density functional theory calculations. The structure and properties of the CH$_2$I–I species and the CH$_2$I$_2$···I molecular complex and their reaction towards ethylene were compared. The CH$_2$I–I species and the CH$_2$I$_2$···I both have weak I–I bonds that are the chromophores responsible for similar intense transient absorption bands. However, the geometry of the I–I bond relative to the C–I bond is noticeably different for these two species and this leads to distinctly different chemical reactivity toward carbon double bonds. The CH$_2$I–I isomer readily reacts with ethylene to produce a cyclopropane product and I$_2$ leaving group via a single step and low barrier to reaction while the CH$_2$I$_2$···I molecular complex reacts with ethylene to form an ethylene/I intermediate and a CH$_2$I$_2$ leaving group. Probable ramifications for other related molecule–halogen atom complexes are briefly discussed. © *2002 American Institute of Physics.*
[DOI: 10.1063/1.1511724]

I. INTRODUCTION

The photochemistry and chemistry of polyhalomethane molecules have long been an active subject of investigation from several viewpoints. A number of polyhalomethane molecules such as CH$_2$I$_2$, CH$_2$Br$_2$, CH$_2$C1I, CH$_2$BrI, CHBr$_3$ and others have been observed in the troposphere and are thought to be important sources of reactive halogens in the atmosphere.[1–8] Some polyhalomethanes have also found utility as reagents for the cyclopropanation of olefins and diiodomethylation of carbonyl compounds in synthetic chemistry.[9–16] For example, the ultraviolet photoexcitation of CH$_2$I$_2$ in the presence of olefins in room temperature solutions can be used to produce cyclopropanated products in reasonably good yields with high stereospecificity.[10,11,13] Polyhalomethane molecules have also been useful molecules to study in order to better understand fundamental aspects of photodissociation reactions.[17–33]

Ultraviolet photolysis of polyhalomethanes in the gas phase typically leads to a direct carbon–halogen bond cleavage reaction.[17–33] Molecular beam anisotropy measurements indicate these reactions occur in time much less than a rotational period of the parent molecule.[17,19,22–26,29,31] Time-of-flight photofragment spectroscopy experiments for several polyhalomethanes indicate that the polyatomic fragments usually receive substantial degrees of internal excitation of their rotational and/or vibrational degrees of freedom.[19,22–26,29] Resonance Raman studies of a range of polyhalomethanes showed that the photodissociation reactions typically had significant multidimensional character and short-time dynamics qualitatively consistent with a semi-rigid radical description of the dissociation in both gas and solution phases.[34–43]

Ultraviolet excitation of polyhalomethanes in condensed phase environments leads to production of photoproduct(s) that have characteristic transient absorption bands in the ultraviolet and visible regions that were tentatively assigned to be due to a range of possible species such as cations, radicals, and/or isomer products.[44–50] Recent femtosecond transient absorption experiments suggest these species are formed by geminate recombination of the fragments within the solvent cage.[51–55] Time-resolved resonance Raman experiments in conjunction with density functional theory cal-

culations for proposed photoproduct species demonstrated that polyhalomethane isomer products (isopolyhalomethanes) were mostly responsible for the ultraviolet transient absorption bands observed on the picosecond and nanosecond time scales in liquid solutions.[56–63]

Both theory and experiment were recently used to examine the chemical reactivity of isopolyhalomethanes toward olefins.[64–68] The chemical reactivity of isodiiodomethane ($CH_2I–I$), the CH_2I radical and the CH_2I^+ cation species toward ethylene was investigated using density functional theory calculations.[64] This study showed the $CH_2I–I$ species easily reacts with ethylene to produce a cyclopropane product and I_2 leaving group via a one-step reaction with a barrier height of about 2.9 kcal/mol.[64] However, the CH_2I radical and CH_2I^+ cation species have much more difficult reactions with ethylene to make a cyclopropane product via a two step mechanism that forms relatively stable iodopropyl radical or iodopropyl cation intermediates and have much greater barriers to reaction for the rate-determining step to form cyclopropane than the $CH_2I–I$ species.[64] The reaction of $CH_2I–I$ with cyclohexene was directly probed using time-resolved resonance Raman spectroscopy (TR^3) experiments[66] under conditions similar to the original photochemical studies of Blomstrom, Herbig and Simmons[10] that found significant conversion of CH_2I_2 into the norcarane product (e.g., the cyclopropanated product of cyclohexene).[10] These TR^3 experiments demonstrated that $CH_2I–I$ reacts with cyclohexene on the 5–10 ns time scale and then almost immediately forms a I_2: cyclohexene complex.[66] This in conjunction with the results from the density functional theory calculations indicates that $CH_2I–I$ is the carbenoid (or methylene transfer agent) mostly responsible for the cyclopropanation of olefins when utilizing the ultraviolet photolysis of CH_2I_2. Further experimental and theoretical work indicates that a number of isopolyhalomethanes can act as carbenoids with varying degrees of reactivity towards carbon double bonds.[65,67,68]

TR^3 experiments indicate that the $CH_2I–I$ isomer species decays fairly fast in cyclohexane solution (on the order of tens of nanoseconds and there is almost no $CH_2I–I$ signal by 80–100 ns)[66] while some pulse radiolysis and laser flash photolysis experiments for a number of iodoalkanes[69–73] observed a transient absorption spectrum on the microsecond time scale that is very similar to that observed for $CH_2I–I$ on the picosecond to nanosecond time scales.[51–53] In this paper, we report TR^3 experiments done at different concentrations of CH_2I_2 in cyclohexane solution. At low concentration we mainly observe the $CH_2I–I$ species and see it decay on the order of tens of nanoseconds to almost no signal at 100 ns and nothing else is observed up to 15 microseconds. At high concentration we observe spectra from two species. The first species is $CH_2I–I$ and its spectra and decay are essentially identical to that found at low concentration of CH_2I_2 parent molecule. The second species is a $CH_2I_2\cdots I$ molecular complex that appears to be formed from bimolecular reaction of iodine atoms with CH_2I_2 molecules. Density functional theory computations are used to explore the chemical reactivity of the $CH_2I–I$ species and the $CH_2I_2\cdots I$ molecular complex. We compare the structure and properties of the $CH_2I–I$ species and the $CH_2I_2\cdots I$ molecular complex and

their reaction towards ethylene. Our results indicate that both the $CH_2I–I$ species and the $CH_2I_2\cdots I$ molecular complex have loosely bound I–I bonds that give rise to similar strong transient absorption bands. However, their structures are noticeably different (especially for the geometry of the I–I bond relative to the C–I bond) and this leads to distinctly different chemical reactivity toward carbon double bonds. We briefly discuss implications for other related molecule–halogen atom complexes.

II. EXPERIMENT AND CALCULATIONS

Samples of CH_2I_2 (99%) were prepared with 0.25 M and 0.62 M concentrations in spectroscopic grade cyclohexane solvent. The nanosecond time-resolved resonance Raman (TR^3) experimental apparatus and methods have been detailed elsewhere[66,68] so only a brief description will be given here. The pump (266 nm) and probe (416 nm) excitation wavelengths were obtained from the fourth harmonic and the first Stokes hydrogen Raman shifted laser line of the third harmonic of two nanosecond pulsed Nd:YAG lasers (Spectra Physics GCR-150-10 and LAB-170-10). A pulse delay generator (Stanford Research Systems) was used to set and synchronize the firing of both the flashlamps and Q-switches of the two lasers in order to control the relative timing of the pump and probe laser pulses. A fast photodiode and its output displayed on a 500 MHz oscilloscope (Hewlett-Packard) was used to measure the relative timing between the two laser pulses.

The pump and probe laser beams were loosely focused onto a flowing liquid stream of sample using a near-collinear and backscattering geometry. Reflective optics were used to collect the Raman scattered light and image it through a depolarizer and entrance slit of a 0.5 meter spectrograph whose grating dispersed the light onto a liquid nitrogen cooled CCD detector. The CCD collected signal for about 300 s before being readout to an interfaced PC computer and 5 to 10 of these readouts were summed to obtain a spectrum at each time delay. For each time delay, a probe only spectrum, a pump only spectrum in the probe wavelength region, and a pump–probe spectrum were obtained. A background scan was also acquired before and after each experimental trial. The known vibrational frequencies of the cyclohexane solvent Raman bands were used to calibrate the Raman shifts of the resonance Raman spectra. Probe only and pump only spectra were subtracted from the pump–probe spectra so as to remove solvent and parent Raman bands and obtain the time-resolved resonance Raman spectra.

The reactions of the $CH_2I–I$ isomer species and the $CH_2I_2\cdots I$ molecular complex with ethylene were investigated using density functional theory calculations. The stationary structures were fully optimized using C_1 symmetry and B3LYP theory[74–78] and the 6-311G^{**}, TZVP[81] and/or Sadlej-pVTZ basis sets.[79–81] Analytical frequency computations were performed to confirm the optimized structure to be a minimum or first-order saddle point and to also find the zero-point energy correction. Intrinsic reaction coordinate (IRC) calculations[82] were also performed to confirm the transition states connected the related reactants and products and
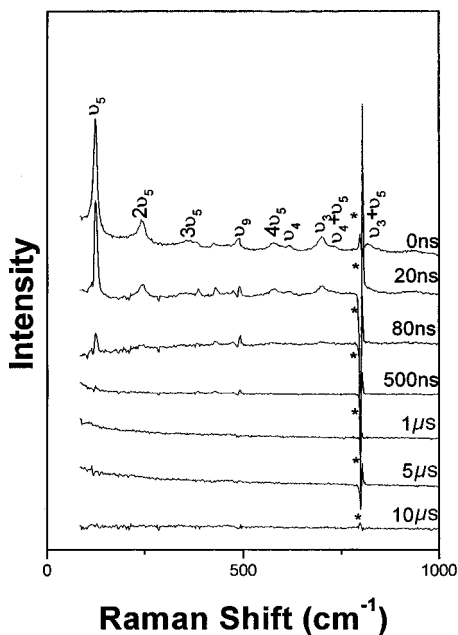
FIG. 1. Overview of 416 nm time-resolved resonance Raman spectra obtained after 266 nm photolysis of 0.25 M CH$_2$I$_2$ in cyclohexane solution. Spectra are shown for time delays of about 0, 20, 80, and 500 ns, and 1, 5, and 15 μs. The assignments of the larger Raman bands for the CH$_2$I–I isomer are shown above the spectra (see text and Table II). The asterisks mark regions where solvent/parent subtraction artifacts are present and the daggers label stray light or ambient light artifacts.
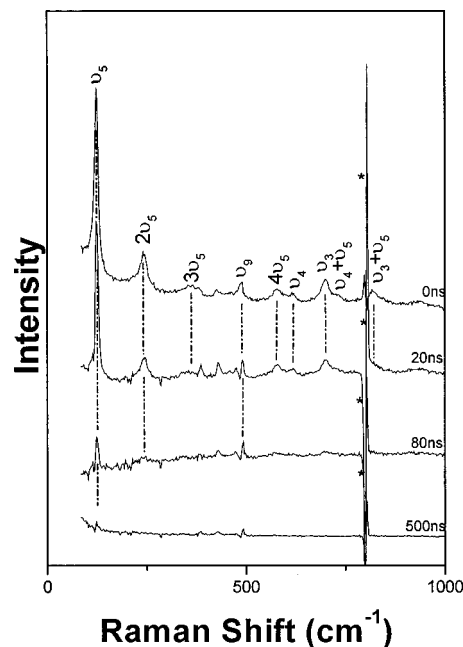

FIG. 2. Expanded view of the time-resolved resonance Raman spectra of Fig. 1 for time delays of 0, 20, 80, and 500 ns. The assignments of the larger Raman bands for the CH$_2$I–I isomer are shown above the spectra (see text and Table II). The asterisks mark regions where solvent/parent subtraction artifacts are present and the daggers label stray light or ambient light artifacts.

to characterize the reaction coordinate. The GAUSSIAN 98W program suite[83] was used for all of the calculations.

III. RESULTS AND DISCUSSION

A. Time-resolved resonance Raman spectra, density functional theory computational results, and assignment of CH$_2$I–I and CH$_2$I$_2$···I species to the time-resolved resonance Raman spectra

Figure 1 shows time-resolved resonance Raman spectra obtained after 266 nm photolysis of 0.25 M CH$_2$I$_2$ in cyclohexane solution at delay times ranging from about 0 ns to 10 μs. Figure 2 presents an expanded view of the 0 ns, 20 ns, 80 ns and 500 ns spectra of Fig. 1. The spectra observed at 0 ns, 20 ns and 80 ns in Figs. 1 and 2 are in very good agreement with those obtained in earlier studies using similar concentrations of CH$_2$I$_2$ in cyclohexane solvent.[56,57,66] The Raman bands observed in Figs. 1 and 2 are mainly due to the CH$_2$I–I isomer species. The larger CH$_2$I–I isomer Raman bands include the nominal I–I stretch fundamental (v_5) at ~123 cm^{-1} and its overtones ($2v_5$ and $3v_5$), the nominal C–I stretch fundamental (v_3) at ~698 cm^{-1}, and the nominal CH$_2$ wag fundamental (v_4) at ~620 cm^{-1}. Table I presents selected optimized geometry parameters for the CH$_2$I–I species from previous density functional theory calculations.[56,64] Table II compares the experimental Raman vibrational band frequencies to those predicted from previous density functional theory calculations and the reader is referred to Ref. 56 for more details of the Raman band assignment to the CH$_2$I–I isomer product.

Figure 3 presents time-resolved resonance Raman spectra obtained after 266 nm photolysis of 0.62 M CH$_2$I$_2$ in

cyclohexane solution at delay times ranging from about 0 ns to 15 μs. Figure 4 gives an enlarged view of the 0, 10, 20, and 80 ns, and 15 μs spectra of Fig. 3. Comparison of the spectra shown in Figs. 3 and 4 to those in Figs. 1 and 2 shows that there are clearly two species seen after photolysis of higher CH$_2$I$_2$ concentrations in Figs. 3 and 4. The first species observed in the 0, 10, and 20 ns spectra of Figs. 3 and 4 are clearly the CH$_2$I–I isomer species that are also seen in the lower concentration spectra of Figs. 1 and 2 at the same delay times. The appearance of the second species has a very strong dependence on the concentration of CH$_2$I$_2$ used in the experiments and the second species has a significantly longer lifetime on the order of microseconds. This suggests the second species may be formed from a bimolecular reaction and not from a geminate recombination process as was mostly the case for the CH$_2$I–I species. Several previous laser flash photolysis and pulse radiolysis studies of iodoalkanes have observed transient absorption spectra on the nanosecond to microsecond time scale with an absorption maximum around 390 nm[69–73] similar to that observed for the CH$_2$I–I species on the picosecond to nanosecond time scales.[51–53] These longer lived transient absorption bands were assigned to iodoalkane–iodine molecular complexes like the CH$_3$I···I species for the case of photolysis of CH$_3$I in solutions.[69,73] These iodoalkane–iodine molecular complexes were thought to be formed from bimolecular reaction of I atoms (that escape the solvent cage associated with the initially produced CH$_3$ and I fragments) with an iodoalkane molecule. Thus, we suspect that the second species observed in Figs. 3 and 4 is the analogous CH$_2$I$_2$···I molecular complex. We have done density functional theory calculations for this species to estimate its structure and vibrational frequen-

TABLE I. Parameters for the optimized geometry computed from the B3LYP density functional theory computations for the $CH_2I–I$ isomer and the $CH_2I_2\cdots I$ molecular complex proposed as photoproduct species formed following ultraviolet excitation of CH_2I_2 in cyclohexane solution. Bond lengths are in Å and bond angles are in degrees.

Parameter	B3LYP Calc.			B3LYP Calc.
$CH_2I–I$ isomer	TZVP[a]	Sadlej-pVTZ[b]	$CH_2I_2\cdots I$ molecular complex	Sadlej-pVTZ
C–I	1.957	1.968	$C–I_1$	2.144
I–I	3.042	3.019	$C–I_2$	2.166
C–H	1.091	1.093	$I_2–I_3$	3.357
C–I–I	118.2	121.8	$C–I_3$	3.774
I–C–H	119.1	118.1	C–H	1.093
D(H–C–I–I)	90	78.8	$I_1–C–I_2$	115.1
			$C–I_2–I_3$	83.2
			$I_1–C–H$	108.7
			$I_2–C–H$	106.4
			$D(I_1–C–I_2–I_3)$	173.5

[a]Values from Ref. 56.
[b]Values from Ref. 64.

cies (shown in Tables I and II, respectively). The second species time resolved vibrational frequencies in Figs. 3 and 4 are in excellent agreement with those predicted by the B3LYP computed values shown in Table II. This indicates the second species is most likely indeed the $CH_2I_2\cdots I$ molecular complex and its Raman band vibrational frequencies can be assigned as follows: the strong band at 118 cm^{-1} is assigned to the nominal I–C–I bend mode (v_9) that is computed to be at 118 cm^{-1}; the Raman band at 486 cm^{-1} is assigned to the nominal I–C–I symmetric stretch (v_8) com-

puted to be at 487 cm^{-1}; the Raman band at 574 cm^{-1} is assigned to the nominal I–C–I antisymmetric stretch (v_7) computed to be at 582 cm^{-1}.

B. Comparison of the structures of $CH_2I–I$ and $CH_2I_2\cdots I$ species and their chemical reactivity toward ethylene

Figure 5 displays schematic diagram of the computed optimized geometry determined from the B3LYP/6-311G**

TABLE II. Comparison of experimental vibrational frequencies (in cm^{-1}) found for the two species observed in the time-resolved resonance Raman (TR^3) spectra of Figs. 1–4 to the B3LYP calculated vibrational frequencies for the species whose optimized geometry is given in Table I.

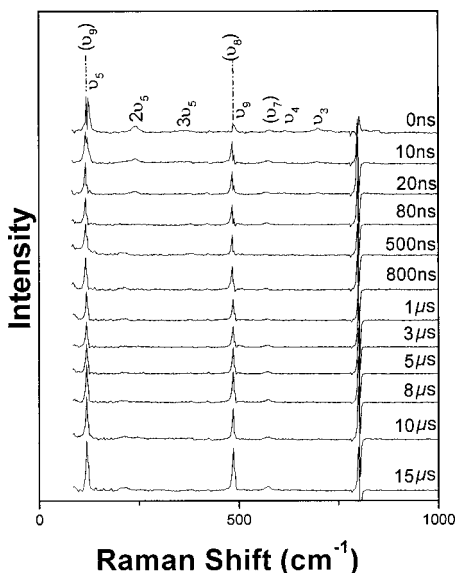| Vibrational mode	B3LYP Calc.	TR^3 spectra Vibrational frequency (in cm^{-1})	
$CH_2I–I$ isomer	TZVP (from Ref. 56)	First species (see in Figs. 1–4)	
Possible assignment		This work	From Ref. 56
$A'v_1$, C–H sym. stretch	3131		
v_2, C–H$_2$ scissor	1340		
v_3, C–I stretch	755	698	701
v_4, CH$_2$ wag	619	620	619
v_5, I–I stretch	128	123	128
v_6, C–I–I bend	99		
$A''v_7$, C–H asym. stretch	3281		
v_8, CH$_2$ rock	865		
v_9, CH$_2$ twist	447	491	487
$CH_2I_2\cdots I$ molecular complex	Sadlej-pVTZ (this work)	Second species (seen in Figs. 3 and 4)	
Possible assignment		This work	
$A'v_1$, C–H asym. stretch	3207		
v_2, C–H sym. strech	3111		
v_3, H–C–H bend (in plane)	1376		
v_4, H–C–H bend (o.p.) sym.	1116		
v_5, H–C–H bend (o.p.) asym.	1040		
v_6, CH$_2$ rock	707		
v_7, $I_1–C–I_2$ asym. stretch	582	574	
v_8, $I_1–C–I_2$ sym. stretch	487	486	
v_9, $I_1–C–I_2$ bend (in plane)	118	118	
v_{10}, $I_2–I_3$ stretch	76		
v_{11}, $I_1–C–I_2$ bend (o.p.)	47		
v_{12}, $C–I_3$ stretch+H–C–H asym. bend	31		

FIG. 3. Overview of 416 nm time-resolved resonance Raman spectra obtained after 266 nm photolysis of 0.62 M CH$_2$I$_2$ in cyclohexane solution. Spectra are shown for time delays of about 0, 10, 20, 80, 500, and 800 ns, and 1, 3, 5, 8, 10, and 15 μs. The assignments of the larger Raman bands to the CH$_2$I–I isomer and the CH$_2$I$_2\cdots$I molecular complex are shown above the spectra (see text and Table II). The assignments for the CH$_2$I$_2\cdots$I molecular complex are shown in parentheses. The asterisks mark regions where solvent/parent subtraction artifacts are present and the daggers label stray light or ambient light artifacts.

computations for the CH$_2$I–I isomer, the CH$_2$I radical and CH$_2$I$_2\cdots$I molecular complex species as well as the transition state(s) for the reaction of these species with ethylene. The Cartesian coordinates, total energies and vibrational zero-point energies for selected stationary structures given in
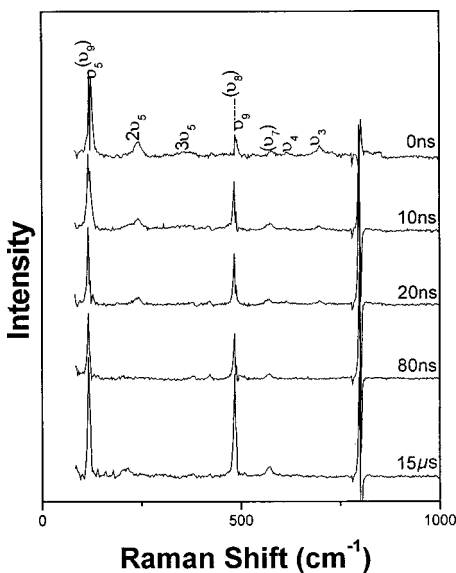

FIG. 4. Expanded view of the time-resolved resonance Raman spectra of Fig. 1 for time delays of 0, 10, 20, and 80 ns, and 15 μs. The assignments of the larger Raman bands to the CH$_2$I–I isomer and the CH$_2$I$_2\cdots$I molecular complex are shown above the spectra (see text and Table II). The assignments for the CH$_2$I$_2\cdots$I molecular complex are shown in parentheses. The asterisks mark regions where solvent/parent subtraction artifacts are present and the daggers label stray light or ambient light artifacts.

Fig. 5 are available in the supporting information.[84] Comparison of the structures shown in Fig. 5 and geometry parameters presented in Table I for the CH$_2$I–I isomer species and the CH$_2$I$_2\cdots$I molecular complex reveals that they have some similarities as well as significant differences in their structures. Both species contain a loosely bound I–I bond that is somewhat weaker in the CH$_2$I$_2\cdots$I molecular complex (3.357 Å) compared to the CH$_2$I–I isomer species (3.019 Å). This difference in the I–I bond is accompanied by significant differences in other parts of the structures. For example, the C–I–I angle is substantially different in the two species with a value of about 122° for the CH$_2$I–I species compared to about 83.7° for the CH$_2$I$_2\cdots$I molecular complex. This difference in the C–I–I angle leads to a small but noticeable interaction between the C atom and the loosely bound terminal I atom (C–I distance of 3.788 Å and contributes to the low frequency mode v_{12} at 31 cm^{-1}) for the CH$_2$I$_2\cdots$I molecular complex. This interaction is essentially absent in the CH$_2$I–I isomer species. We note that the structures for the isomers of a range of polyhalomethanes have C–X–X or C–Y–X angles in the 115° to 150° range[56,58–62,64,65] and this suggests that the terminal halogen atom of the halogen–halogen bond has little direct interaction with the carbon atom for isopolyhalomethanes. The C–I bond lengths are noticeably different with the CH$_2$I–I isomer species (1.968 Å) being noticeably stronger than those in the CH$_2$I$_2\cdots$I molecular complex (2.161 Å and 2.144 Å) which are close to those of the parent CH$_2$I$_2$ molecule. These results suggest the C–I bonds are only modestly perturbed by the I–I bonding in the CH$_2$I$_2\cdots$I molecular complex compared to the parent CH$_2$I$_2$ molecule while the CH$_2$I–I isomer species experiences substantially stronger perturbation of its C–I bond due to the I–I bond formation. The I–C–H angles are in the 106.4° to 108.7° range for the CH$_2$I$_2\cdots$I molecular complex and consistent with the C atom having sp^3 bonding character as in the CH$_2$I$_2$ parent molecule. However, the CH$_2$I–I isomer has I–C–H angles of about 118.1° and more consistent with the C atom having sp^2 bonding character.

The DFT calculations found the HOMO of the CH$_2$I$_2\cdots$I molecular complex to be $0.06^2S(C) + 0.038^2P_y(C) - 0.128^5S(I_2) + 0.435^5P_x(I_2) + 0.215^5P_y(I_2) + 0.094^5P_x(I_1) - 0.218^5P_y(I_1) + 0.039^1S(H_4) - 0.044^1S(H_5) + 0.090^5S(I_3) + 0.552^5P_x(I_3) + 0.421^5P_y(I_3)$. The greatest contribution comes from the I$_2$ and I$_3$ atoms and is consistent with the I$_2$–I$_3$ bond formation. There are also smaller contributions from the C atom and the I$_1$ atoms suggesting that there is also some modest interaction between these atoms and the I$_2$–I$_3$ bond formation. This is consistent with the C atom interaction with the I$_3$ atom and its contribution to the low frequency mode v_{12} at 31 cm^{-1} for the CH$_2$I$_2\cdots$I molecular complex. The DFT computations found the HOMO of the CH$_2$I–I isomer species to be $-0.234^5P_z(I_2) + 0.745^5P_z(I_3) + 0.069^1S(H_4) - 0.042^1S(H_5)$ and this is consistent with the I–I bond formation.

The I–I bond formation leads to little changes in the C–I bond lengths and I–C–H bond angles in the CH$_2$I$_2\cdots$I molecular complex compared to the parent CH$_2$I$_2$ molecule. This suggests the charge distribution and chemical reactivity of the CH$_2$I$_2\cdots$I molecular complex will be close to that of a

H_1-C_1-I_1-I_2=-78.3 (-78.8)
H_2-C_1-I_1-I_2=78.3 (78.8)

117.9 (118.1)   123.3 (121.8) I_2 3.045 (3.019)
1.081 (1.093) C_1 1.981 (1.968) I_1
H_2 H_1

TS1
143.5 (142.0) I_2 3.063 (3.044)
2.097 (2.071) H_2 H_1 C_1 I_1
117.0 (117.2)
I_2-I_1-C_1-C_2=180.0
I_1-C_1-C_2-C_3=180.0
2.266 (2.280)
95.7 (96.8) H_5 C_3 1.352 (1.355) C_2 H_3 H_4 H_6

H_6 H_5 114.2 (114.6)
C_3
118.1 (117.9)   60.0 (60.0)   1.083 (1.092)
C_1 1.508 (1.510) C_2 H_4 H_3
H_2 H_1

IM (CH$_2$I radical)
H_2 123.0 (123.0) C_1 2.066 (2.052) I_1
1.090 (1.078) H_1

TS2
H_2 H_1 C_1 2.117 (2.096) I_1
I_1-C_1-C_2-C_3=180.0
106.9 (107.2)   2.308 (2.328)
H_5 C_3 1.355 (1.359) C_2 H_3 H_4 H_6

IM
H_6 H_5
C_2 (1.536)
(1.490) 1.490   109.6 (109.7)   1.538 112.6 (112.9) I_1
H_2 C_3 H_1 C_1 2.209 (2.188) H_3 H_4

TS3
H_6 H_5
C_2 (1.502)
(1.466) 1.466   81.8 (80.8) 1.501   107.4 (107.1) I_1
H_2 C_3 H_1 1.942 (1.923) C_1 2.603 (2.596) H_3 H_4

I_2 3.396 (3.357) I_3
2.179 (2.161)   83.9 (83.7)
I_1 C_1 H 2.159 (2.144) H

TS4
I_3 2.737 I_2
4.520
H C_1 2.118 I_1
H 2.309
H C_3 106.6 C_2 H
H 1.355 H
I_3
3.148
H C_2 H
H 1.343 C_3 H

TS5
I_1
2.164
H C_1 H
2.171
I_2
3.924
I_3 3.722
3.801
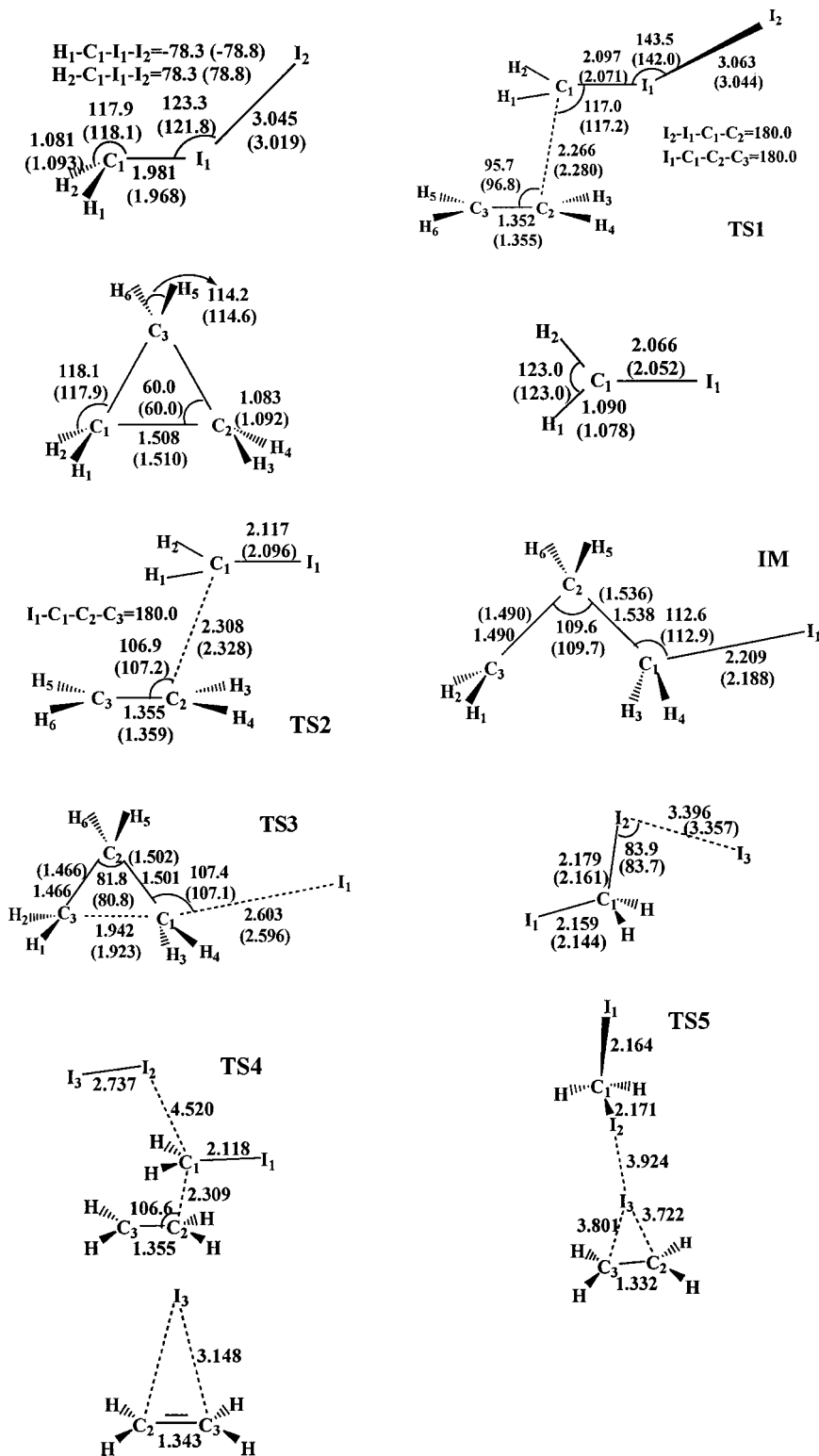H C_3 1.332 C_2 H
H H

FIG. 5. Schematic diagram of the computed optimized geometry determined from the B3LYP/6-311G** computations for the CH$_2$I–I isomer, the CH$_2$I radical and CH$_2$I$_2$···I molecular complex species as well as the transition state(s) for the reaction of these species with ethylene. TS1 = transition state for reaction of CH$_2$I–I with ethylene. TS2 = transition state for reaction of CH$_2$I radical to produce an iodopropyl radical (IM). TS3 = transition state for reaction of the iodoproyl radical to form a cyclopropane product and I atom leaving group. TS4 = transition state for reaction of CH$_2$I$_2$···I molecular complex with ethylene to produce an iodopropyl radical (IM). TS5 = transition state for reaction of CH$_2$I$_2$···I molecular complex with ethylene to produce an ethylene/I species and CH$_2$I$_2$ leaving group. Selected structural parameters are shown for each species with the bond lengths in Å and the bond angles in degrees. Values for the reactions of the CH$_2$I–I isomer and the CH$_2$I radical are from Ref. 64. The values given in parentheses are those found using the Sadlej-pVTZ basis set.

CH$_2$I$_2$ molecule with an I atom nearby. In contrast, the I–I bond formation in the CH$_2$I–I isomer leads to significant changes in the C–I bond compared to either the parent CH$_2$I$_2$ molecule or the CH$_2$I radical. The difference between the parent CH$_2$I$_2$ molecule and CH$_2$I–I isomer may be expected because the C atom has sp^3 bonding in the CH$_2$I$_2$ parent molecule compared to sp^2 bonding in the CH$_2$I–I isomer. However the C atom in both the CH$_2$I–I isomer and the CH$_2$I radical have both sp^2 bonding but the C–I bond is still significantly shorter and stronger in the CH$_2$I–I isomer (1.968 Å) compared to the CH$_2$I radical (2.052 Å).[64] This leads the CH$_2$I–I isomer to have a significantly different charge distribution than that found in the CH$_2$I radical and the CH$_2$I$_2$ parent molecule.[64] The CH$_2$I–I species has a CH$_2$I$^+$I$^-$ radical ion pair character and very different chemical reactivity towards C=C bonds than the CH$_2$I radical or the CH$_2$I$_2$ molecule.[64] Previous density functional theory calculations demonstrated that the CH$_2$I–I isomer readily re-

acts with ethylene to give a cyclopropane product and I$_2$ molecule leaving group via a one step reaction with a small barrier of about 2.9 kcal/mol.[64] However, the CH$_2$I radical reacts with ethylene via a barrier of about 5.2 kcal/mol to produce an iodopropyl radical that is difficult to produce a cyclopropane product and I atom leaving group via a large barrier of about 13.5 kcal/mol.[64] Similarly the CH$_2$I$^+$ cation reacts with little or no barrier to give a relatively stable iodopropyl cation that is even more difficult to undergo ring closure to produce a cyclopropane molecule or cyclopropane cation via large barriers of 96.7 kcal/mol and 35.9 kcal/mol, respectively.[64] This work and further experimental work indicates the CH$_2$I–I isomer is the species mainly responsible for production of cyclopropanated products from olefins when using ultraviolet photolysis of CH$_2$I$_2$ in the presence of olefins.[64,66] We have done similar density functional theory calculations for the reactions of the CH$_2$I$_2 \cdots$I molecular complex with ethylene. The optimized geometry for the reactants, transition states, intermediates and products for these reactions are shown in Fig. 5 and the computed relative energies (in kcal/mol) for these reactions are shown in Fig. 6. We have also included the CH$_2$I–I isomer reaction with ethylene optimized geometry and relative energies from our previous work in Figs. 5 and 6 for comparison purposes.[64] We note the structures, vibrational frequencies and energies are only modestly affected upon changing the basis set from the Sadlej-pVTZ to the smaller 6-311G** for the CH$_2$I–I isomer and its reaction with ethylene.[64] Since the CH$_2$I$_2 \cdots$I molecular complex contains three I atoms and is noticeably more computationally demanding, we have used the 6-311G** basis set for the B3LYP calculations for the reaction of the CH$_2$I$_2 \cdots$I molecular complex with ethylene given in Figs. 5 and 6.

Inspection of Fig. 6 shows that the CH$_2$I$_2 \cdots$I molecular complex reaction with ethylene can break the weak I–I bond to produce an ethylene/I species and an CH$_2$I$_2$ leaving group relatively easily with a small barrier to reaction of about 3.2 kcal/mol. The CH$_2$I$_2 \cdots$I molecular complex can also react with ethylene to break the stronger C–I bond to from an iodopropyl radical intermediate and an I$_2$ leaving group via a large barrier of about 21.4 kcal/mol. This iodopropyl radical intermediate can then proceed to produce a cyclopropane product and I atom leaving group via a barrier of about 12.1 kcal/mol. It is very hard for the CH$_2$I$_2 \cdots$I molecular complex to break a C–I bond when it reacts with ethylene to produce the iodopropyl radical intermediate or proceed to produce a cyclopropane product. This is very different than the CH$_2$I–I isomer species that very easily reacts with ethylene via a one step mechanism and small barrier of about 2.9 kcal/mol to make a cyclopropane product and I$_2$ leaving group.[64] Our results indicate that the CH$_2$I$_2 \cdots$I molecular complex will mostly react with ethylene to transfer the terminal I atom to form an ethylene/I species and a CH$_2$I$_2$ leaving group. This is similar to the reaction of an I atom with ethylene and consistent with the CH$_2$I$_2 \cdots$I molecular complex structure being only modestly different from that of the CH$_2$I$_2$ parent molecule.

Comparison of TS2 and TS4 in Fig. 5 reveals some interesting similarities: the CCC angle is about the same
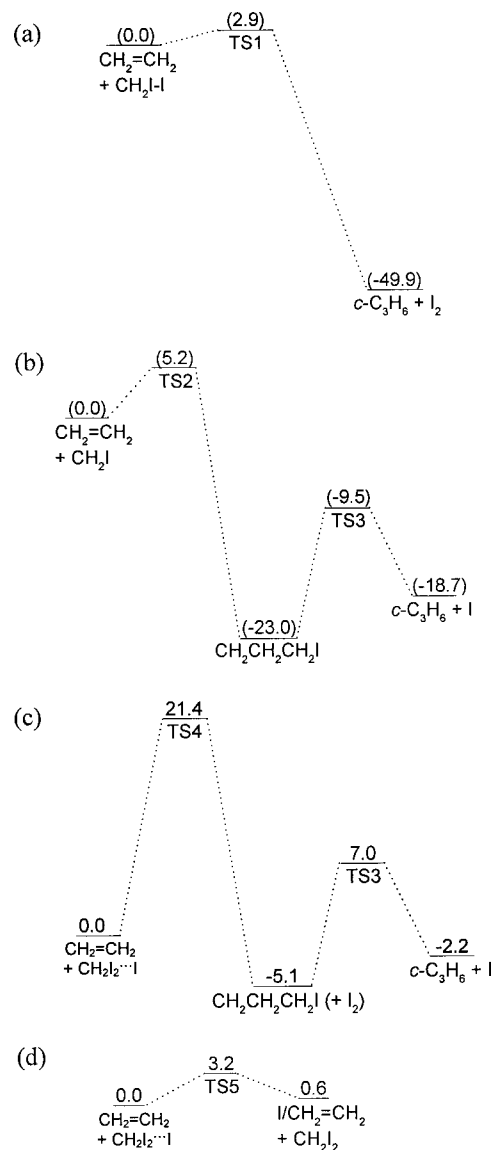

FIG. 6. Schematic diagram showing the computed relative energies (in kcal/mol) for reactions of the CH$_2$I–I isomer (a), the CH$_2$I radical (b), and the CH$_2$I$_2 \cdots$I molecular complex species with ethylene [reactions (c) and (d)] with the transition state, intermediate, and product energies given relative to the separated reactants. Values for reactions (a) and (b) are those from B3LYP/Sadlej-pVTZ computations of Ref. 64. Values for reactions (c) and (d) are those from B3LYP/6-311G** calculations of this work (see text for more details).

(106.9° and 106.6°, respectively), the ethylene C=C bond length is the same (1.355 Å), the C$_1$–C$_2$ bond length is about the same (2.308 Å and 2.312 Å, respectively) and the C–I bond length is about the same (2.117 Å and 2.118 Å, respectively). This indicates the CH$_2$I$_2 \cdots$I molecular complex reaction with ethylene to form the iodopropyl radical intermediate is very similar to the reaction of the CH$_2$I radical with ethylene.[64] This also indicates the larger barrier to reaction of about 21.4 kcal/mol for the CH$_2$I$_2 \cdots$I molecular complex compared to the lower barrier of about 5.2 kcal/mol[64] for the CH$_2$I radical to form the iodopropyl radical intermediate is mainly due to the need to break the strong C–I bond of the CH$_2$I$_2 \cdots$I molecular complex which is lengthened to 4.567 Å in TS4 compared to about 2.179 Å in the CH$_2$I$_2 \cdots$I com-

plex. The strengthening of the I–I bond from 3.396 Å in the $CH_2I_2\cdots I$ complex to about 2.736 Å in TS4 is not enough to compensate the energy needed to break the C–I bond and TS4 is much higher than TS2.

Comparison of the chemical reactivity of the $CH_2I_2\cdots I$ molecular complex, the CH_2I radical and the $CH_2I–I$ isomer species with ethylene reveals that several factors contribute to the very different and remarkable reactivity of the $CH_2I–I$ isomer toward C=C bonds. First, the greater perturbation of the C–I bond in the $CH_2I–I$ isomer by the I–I bond formation leads the $CH_2I–I$ isomer to have a significantly different charge distribution than found in the CH_2I radical, the CH_2I_2 parent molecule or the $CH_2I_2\cdots I$ molecular complex. This leads to the $CH_2I–I$ species having a $CH_2I^+I^-$ radical ion pair character and activates the CH_2I moiety (e.g., like a CH_2I^+ cation that readily reacts with ethylene).[64] Second, the sp^2 bonding character of the C atom in the $CH_2I–I$ isomer or the CH_2I radical compared to the sp^3 bonding character of the C atom in the $CH_2I_2\cdots I$ molecular complex means that a C–I bond does not need to be almost completely broken as in TS4 for the $CH_2I_2\cdots I$ molecular complex reaction with ethylene in order to have the C atom added to the C=C bond. This leads to lower barriers for the $CH_2I–I$ isomer or the CH_2I radical to add to the C=C bond of ethylene. Third, the transition state structure TS1 which has a smaller CCC angle around 95°–97° and the radical ion pair character for the $CH_2I–I$ isomer species appear to combine to give a concerted ring closure so that the $CH_2I–I$ isomer is a very effective methylene transfer agent (e.g., carbenoid species). The radical ion pair character of $CH_2I–I$ appears to promote formation of two molecular products rather than ion or radical leaving groups when forming the cyclopropane product. However, the analogous CCC structure in TS2 for the CH_2I radical reaction with ethylene has an angle near 107° (further away from ring closure). The CH_2I radical also lacks the radical ion pair character of the $CH_2I–I$ isomer. Thus, addition of the CH_2I radical to ethylene leads to formation of the relatively stable iodopropyl radical intermediate rather than to directly give a cyclopropane product.

C. Implications for other molecule–halogen complexes and their reactions

The $CH_2I_2\cdots I$ molecular complex appears to be able to relatively easily transfer its terminal I atom of the I–I bond when it reacts with a C=C bond. We also recently observed the $CH_3I\cdots I$ molecular complex using transient resonance Raman spectroscopy and density functional theory calculations suggest that it has a structure similar to that of the $CH_2I_2\cdots I$ molecular complex with a C–I–I angle in the 80°–90° range.[85] We note that similar haloalkane molecule–halogen atom complexes have been observed following pulse radiolysis and/or photolysis of a variety of haloalkanes and polyhaloalkanes.[69–73] In so far as the structures and chemical reactivity of the haloalkane–halogen atom complexes are similar to that of the $CH_2I_2\cdots I$ molecular complex one may expect that these types of complexes will transfer the terminal halogen atom of the halogen–halogen bond in reactions with other molecules but the halogen atom thus transferred

would have a different chemical reactivity than the reaction of a free halogen atom. There is a range of evidence in the literature to support this hypothesis.

Recent studies of free radical chlorination of alkanes in several halogenated solvents found that the tertiary selectivity was enhanced in these types of solvents[86,87] as was previously found for reactions in aromatic and CS_2 solvents.[88–106] This work and other investigations suggested that halogenated solvent–Cl atom molecular complexes were responsible for the enhanced tertiary selectivity for chlorination of alkanes observed in these halogenated solvents.[86,87] A similar CS_2/Cl complex with a characteristic transient absorption band around 370 nm was shown to be responsible for the increased tertiary selectivity in chlorination of alkanes in CS_2 solvent.[106] We recently directly characterized the structure of this CS_2/Cl complex using transient resonance Raman spectroscopy in conjunction with density functional theory calculations.[107] The CS_2/Cl complex was found to have a structure with the Cl atom attached to the S atom of CS_2 (e.g., an S=C=S$\cdots$Cl molecular complex).[107] This S=C=S$\cdots$Cl molecular complex has the Cl atom loosely bound to the S atom and the CS_2 moiety structure is only slightly perturbed from that of the parent CS_2 molecule.[107] This is very similar to the $CH_2I_2\cdots I$ molecular complex where the C–I bonds are only slightly perturbed from that of the parent CH_2I_2 molecule. This suggests the halogenated solvent–Cl atom molecular complexes (responsible for the enhanced tertiary selectivity for chlorination of alkanes observed in halogenated solvents) have structures similar to the $CH_2I_2\cdots I$ and the S=C=S$\cdots$Cl molecular complexes. It is also very likely these halogenated solvent–Cl atom molecular complexes have a chemical reactivity similar to the S=C=S$\cdots$Cl molecular complex that leads to the enhanced tertiary chlorination selectivity of alkanes in halogenated alkane solvents.[86,87]

The differing chemical reactivity for the $CH_2I–I$ species and the $CH_2I_2\cdots I$ molecular complex is consistent with the amount of cyclopropanated product that is formed as the concentration of alkene reactant is varied. For example, Kropp and co-workers found that the yield of cyclopropanated product increased substantially from 16% to 66% to 80% as the concentration of cyclohexene increased from 0.18 to 1.8 to 10 M, respectively, and the CH_2I_2 precursor concentration was kept constant at 0.05 M.[12] At low cyclohexene concentration the longer lifetime of the $CH_2I_2\cdots I$ molecular complex and other long-lived species like the CH_2I radical and I atoms would be more likely to react with cyclohexene to produce additional products and relatively low amounts of cyclopropanated product from reaction with the short-lived $CH_2I–I$ carbenoid species. However, the shorter-lived but more highly reactive $CH_2I–I$ carbenoid species can better compete with the addition reactions of the longer-lived species to produce a higher yield of cyclopropanated product at high cyclohexene concentrations as found in Kropp and co-workers experiments.[12] The chemical reactivity of the $CH_2I_2\cdots I$ molecular complex to mainly transfer an I atom and not produce a cyclopropanated product is also consistent with the chemical reactivity of related halogenated solvent–Cl atom molecular complexes that have

been proposed for being responsible for the enhanced tertiary selectivity for chlorination of alkanes observed in these halogenated solvents.[86,87]

Breslow, Krogh-Jesperson and co-workers showed that the pyridine/Cl complex (responsible for enhanced tertiary selectivity in photochlorination of alkanes in pyridine solvent) is a σ-complex with three-electron–two-center N–Cl bonding.[98] The Cl atom is a highly reactive species with high electronegativity and an unpaired electron in the p-orbital and can therefore easily interact with some types of solvent molecules. A number of radical cations have been shown to form $2\sigma/1\sigma^*$ two-center–three-electron bonds (also known as $2c-3e$ bonds) from the interaction of a singly occupied sulfur p orbital and lone pairs of O, N, P, or halogen atoms.[108–119] These sulfur (or nitrogen, halogen atom) radical cation $2c-3e$ bonded radical cation complexes typically have intense, broad and structureless UV/visible absorption bands[108–119] similar to transient absorption bands observed for isopolyhalomethanes and halogenated solvent–halogen atom complexes that contain the weak halogen–halogen bond as a chromophore.[46,47,51–55,69–73,86,87] The isopolyhalomethanes and halogenated solvent–halogen atom complexes also exhibit weak bond formation from the p-orbital overlap of the two halogen atoms forming the halogen–halogen bond similar to the traditional $2c-3e$ bonded radical cation complexes.[108–119] The actual structure, properties and bond strength of $2c-3e$ bonds (or p-orbital interactions between S, N, O, and/or halogen atoms) are expected to be influenced by the structure and properties of the radical cation or molecule that interacts with the p-orbital of a S, N, O or halogen atom (F, Cl, Br or I) as well as the solvent environment. A range of quantum mechanical calculations have been done to develop a better understanding of $2c-3e$ bonding.[120–133] However, most experimental characterization of $2c-3e$ radical cation bond complexes have been indirect with the transient absorption spectra typically used as an indicator for this kind of bonding and this has made detailed comparisons between theory and experiment somewhat difficult.[108–118] Recently femtosecond spectroscopy has been used to examine a $2c-3e$ bonded sulfur system.[119] Our present comparison of the weak I–I bond in CH$_2$I–I isomer and CH$_2$I$_2\cdots$I molecular complex using time-resolved resonance Raman spectroscopy illustrates the usefulness of time-resolved vibrational spectroscopy to directly characterize the structure and properties of p-orbital interactions similar to $2c-3e$ bonding in neutral species. We anticipate that similar experiments for $2c-3e$ bonded radical cation complexes will enable vibrational mode-specific characterization of these interesting species to be done and allow an even greater understanding of these species to be developed. It will be very interesting to compare the $2c-3e$ bonding in the radical cation complexes to those of the isopolyhalomethane and halogenated solvent–halogen atom complexes that are neutral species.

IV. CONCLUSION

Time-resolved resonance Raman spectra were acquired after ultraviolet photolysis of different concentrations of CH$_2$I$_2$ in cyclohexane solutions. At low concentrations, the CH$_2$I–I isomer species was observed between 0 and 100 ns and no other discernible species was seen up to a 10 μs time delay. At high concentrations, the CH$_2$I–I isomer species was observed with spectra and a lifetime almost identical to that found at lower concentrations and a second species was also observed with a much longer lifetime on the order of microseconds. The second species was assigned to be due to the CH$_2$I$_2\cdots$I molecular complex formed from the bimolecular reaction of I atom with the CH$_2$I$_2$ molecule. Density functional theory calculations were performed to examine the chemical reactivity of the CH$_2$I–I isomer and CH$_2$I$_2\cdots$I molecular complex toward C=C using ethylene as an example. The CH$_2$I–I isomer reacts with ethylene to give a cyclopropane product and I$_2$ leaving group via a one step reaction with a low barrier of about 2.9 kcal/mol. The CH$_2$I$_2\cdots$I molecular complex reacts with ethylene to produce a etheylene/I intermediate and CH$_2$I$_2$ leaving group with a barrier to reaction of about 3.2 kcal/mol. Our results indicate that CH$_2$I–I acts as an effective methylene transfer agent while the CH$_2$I$_2\cdots$I molecular complex essentially transfers the terminal I atom of the I–I bond. This very different chemical reactivity of the CH$_2$I–I and CH$_2$I$_2\cdots$I species can be explained by their differing structures and properties. While both species contain a weak I–I bond, the geometry of the I–I bond relative to the C–I bond is substantially different and leads to greater changes in the case of the CH$_2$I–I species. This leads the CH$_2$I–I species to have a CH$_2$I$^+$I$^-$ radical ion pair character where the CH$_2$I moiety has a charge distribution similar to a CH$_2$I$^+$ cation and thus more easily attacks the C=C bond.[64] The sp^2 bonding character of the C atom in the CH$_2$I–I isomer compared to the sp^3 bonding character of the C atom in the CH$_2$I$_2\cdots$I molecular complex also makes the CH$_2$I–I species more able to form a C–C bond between the C=C bond and the CH$_2$I–I species compared to the CH$_2$I$_2\cdots$I molecular complex which would need to essentially break a C–I bond to do the same. The structure of the CH$_2$I$_2\cdots$I molecular complex is very similar to the parent CH$_2$I$_2$ molecule and this is consistent with its transfer of the terminal I atom of the I–I bond in its reaction with ethylene. We compare our results for the structure and chemical reactivity of the CH$_2$I$_2\cdots$I molecular complex to other halogenated solvent–halogen atom molecular complexes and discuss probable implications for photochlorination reactions of alkanes in halogenated solvents.

[1] Th. Class and K. Ballschmiter, J. Atmos. Chem. **6**, 35 (1988).
[2] S. Klick and K. Abrahamsson, J. Geophys. Res. **97**, 12683 (1992).
[3] K. G. Heumann, Anal. Chim. Acta **283**, 230 (1993).
[4] R. M. Moore, M. Webb, R. Tokarczyk, and R. Wever, J. Geophys. Res., [Oceans] **101**, 20899 (1996).
[5] J. C. Mössinger, D. E. Shallcross, and R. A. Cox, J. Chem. Soc., Faraday Trans. **94**, 1391 (1998).

[6] C. T. McElroy, C. A. McLinden, and J. C. McConnell, Nature (London) **397**, 338 (1999).

[7] L. J. Carpenter, W. T. Sturges, S. A. Penkett, and P. S. Liss, J. Geophys. Res., [Oceans] **104**, 1679 (1999).

[8] B. Alicke, K. Hebstreit, J. Stutz, and U. Platt, Nature (London) **397**, 572 (1999).

[9] H. E. Simmons and R. D. Smith, J. Am. Chem. Soc. **81**, 4256 (1959).

[10] D. C. Blomstrom, K. Herbig, and H. E. Simmons, J. Org. Chem. **30**, 959 (1965).

[11] N. J. Pienta and P. J. Kropp, J. Am. Chem. Soc. **100**, 655 (1978).

[12] P. J. Kropp, N. J. Pienta, J. A. Sawyer, and R. P. Polniaszek, Tetrahedron **37**, 3229 (1981).

[13] P. J. Kropp, Acc. Chem. Res. **17**, 131 (1984).

[14] E. C. Friedrich, S. E. Lunetta, and E. J. Lewis, J. Org. Chem. **54**, 2388 (1989).

[15] S. Durandetti, S. Sibille, and J. Pérchon, J. Org. Chem. **56**, 3255 (1991).

[16] J. M. Concellón, P. L. Bernad, and J. A. Pérez-Andrés, Tetrahedron Lett. **39**, 1409 (1998).

[17] M. Kawasaki, S. J. Lee, and R. Bersohn, J. Chem. Phys. **63**, 809 (1975).

[18] G. Schmitt and F. J. Comes, J. Photochem. **14**, 107 (1980).

[19] P. M. Kroger, P. C. Demou, and S. J. Riley, J. Chem. Phys. **65**, 1823 (1976).

[20] J. B. Koffend and S. R. Leone, Chem. Phys. Lett. **81**, 136 (1981).

[21] S. R. Cain, R. Hoffman, and R. Grant, J. Phys. Chem. **85**, 4046 (1981).

[22] S. J. Lee and R. Bersohn, J. Phys. Chem. **86**, 728 (1982).

[23] L. J. Butler, E. J. Hintsa, and Y. T. Lee, J. Chem. Phys. **84**, 4104 (1986).

[24] L. J. Butler, E. J. Hintsa, and Y. T. Lee, J. Chem. Phys. **86**, 2051 (1987).

[25] E. A. J. Wannenmacher, P. Felder, and J. R. Huber, J. Chem. Phys. **95**, 986 (1991).

[26] G. Baum, P. Felder, and J. R. Huber, J. Chem. Phys. **98**, 1999 (1993).

[27] U. Marvet and M. Dantus, Chem. Phys. Lett. **256**, 57 (1996).

[28] Q. Zhang, U. Marvet, and M. Dantus, J. Chem. Phys. **109**, 4428 (1998).

[29] K.-W. Jung, T. S. Ahmadi, and M. A. El-Sayed, Bull. Korean Chem. Soc. **18**, 1274 (1997).

[30] W. Radloff, P. Farmanara, V. Stert, E. Schreiber, and J. R. Huber, Chem. Phys. Lett. **291**, 173 (1998).

[31] K. Kavita and P. K. Das, J. Chem. Phys. **112**, 8426 (2000).

[32] S. L. Baughcum, H. Hafmann, S. R. Leone, and D. Nesbitt, Faraday Discuss. Chem. Soc. **67**, 306 (1979).

[33] S. L. Baughcum and S. R. Leone, J. Chem. Phys. **72**, 6531 (1980).

[34] J. Zhang and D. G. Imre, J. Chem. Phys. **89**, 309 (1988).

[35] W. M. Kwok and D. L. Phillips, Chem. Phys. Lett. **235**, 260 (1995).

[36] S. Q. Man, W. M. Kwok, and D. L. Phillips, J. Phys. Chem. **99**, 15705 (1995).

[37] W. M. Kwok and D. L. Phillips, J. Chem. Phys. **104**, 2529 (1996).

[38] W. M. Kwok and D. L. Phillips, J. Chem. Phys. **104**, 9816 (1996).

[39] S. Q. Man, W. M. Kwok, A. E. Johnson, and D. L. Phillips, J. Chem. Phys. **105**, 5842 (1996).

[40] F. Duschek, M. Schmitt, P. Vogt, A. Materny, and W. Kiefer, J. Raman Spectrosc. **28**, 445 (1997).

[41] M. Braun, A. Materny, M. Schmitt, W. Kiefer, and V. Engel, Chem. Phys. Lett. **284**, 39 (1998).

[42] X. Zheng and D. L. Phillips, Chem. Phys. Lett. **313**, 467 (1999).

[43] D. L. Phillips, Prog. React. Kinet. **24**, 223 (1999).

[44] J. P. Simons and P. E. R. Tatham, J. Chem. Soc. A **1996**, 854 (1966).

[45] H. Mohan, K. N. Rao, and R. M. Iyer, Radiat. Phys. Chem. **23**, 505 (1984).

[46] G. Maier and H. P. Reisenauer, Angew. Chem. Int. Ed. Engl. **25**, 819 (1986).

[47] G. Maier, H. P. Reisenauer, J. Lu, L. J. Scaad, and B. A. Hess, Jr., J. Am. Chem. Soc. **112**, 5117 (1990).

[48] L. Andrews, F. T. Prochaska, and B. S. Ault, J. Am. Chem. Soc. **101**, 9 (1979).

[49] H. Mohan and R. M. Iyer, Radiat. Eff. **39**, 97 (1978).

[50] H. Mohan and P. N. Moorthy, J. Chem. Soc., Perkin Trans. 2 **2**, 277 (1990).

[51] B. J. Schwartz, J. C. King, J. Z. Zhang, and C. B. Harris, Chem. Phys. Lett. **203**, 503 (1993).

[52] K. Saitow, Y. Naitoh, K. Tominaga, and Y. Yoshihara, Chem. Phys. Lett. **262**, 621 (1996).

[53] A. N. Tarnovsky, J.-L. Alvarez, A. P. Yartsev, V. Sündstrom, and E. Åkesson, Chem. Phys. Lett. **312**, 121 (1999).

[54] A. N. Tarnovsky, M. Wall, M. Rasmusson, T. Pascher, and E. Åkesson, J. Chin. Chem. Soc. (Taipei) **47**, 769 (2000).

[55] A. N. Tarnovsky, M. Wall, M. Gustafsson, N. Lascoux, V. Sundström, and E. Åkesson, J. Phys. Chem. A **106**, 5999 (2002).

[56] X. Zheng and D. L. Phillips, J. Phys. Chem. A **104**, 6880 (2000).

[57] W. M. Kwok, C. Ma, A. W. Parker, D. Phillips, M. Towrie, P. Matousek, and D. L. Phillips, J. Chem. Phys. **113**, 7471 (2000).

[58] X. Zheng and D. L. Phillips, Chem. Phys. Lett. **324**, 175 (2000).

[59] X. Zheng and D. L. Phillips, J. Chem. Phys. **113**, 3194 (2000).

[60] X. Zheng, W. M. Kwok, and D. L. Phillips, J. Phys. Chem. A **104**, 10464 (2000).

[61] X. Zheng, W.-H. Fang, and D. L. Phillips, J. Chem. Phys. **113**, 10934 (2000).

[62] X. Zheng, C. W. Lee, Y.-L. Li, W.-H. Fang, and D. L. Phillips, J. Chem. Phys. **114**, 8347 (2001).

[63] W. M. Kwok, C. Ma, A. W. Parker, D. Phillips, M. Towrie, P. Matousek, X. Zheng, and D. L. Phillips, J. Chem. Phys. **114**, 7536 (2001).

[64] D. L. Phillips, W.-H. Fang, and X. Zheng, J. Am. Chem. Soc. **123**, 4197 (2001).

[65] D. L. Phillips and W.-H. Fang, J. Org. Chem. **66**, 5890 (2001).

[66] Y.-L. Li, K. H. Leung, and D. L. Phillips, J. Phys. Chem. A **105**, 10621 (2001).

[67] W.-H. Fang, D. L. Phillips, D. Wang, and Y.-L. Li, J. Org. Chem. **67**, 154 (2002).

[68] Y.-L. Li, D. M. Chen, D. Wang, and D. L. Phillips, J. Org. Chem. **67**, 4228 (2002).

[69] T. A. Grover and G. Porter, Proc. R. Soc. London, Ser. A **262**, 476 (1961).

[70] J. K. Thomas, J. Phys. Chem. **71**, 1919 (1967).

[71] J. P. Mittal and W. H. Hamill, J. Am. Chem. Soc. **89**, 5749 (1967).

[72] U. Bruhlmann, H. Buchler, F. Marchetti, and R. E. Buhler, Chem. Phys. Lett. **21**, 412 (1973).

[73] L. C. T. Shoute and P. Neta, J. Phys. Chem. **95**, 4411 (1991).

[74] A. D. Becke, J. Chem. Phys. **98**, 1372 (1993).

[75] A. P. Scott and L. Radom, J. Phys. Chem. **100**, 16502 (1996).

[76] S. H. Vosko, L. Wilk, and M. Nusair, Can. J. Phys. **58**, 1200 (1980).

[77] A. D. Becke, Phys. Rev. A **38**, 3098 (1988).

[78] C. Lee, W. Yang, and R. G. Parr, Phys. Rev. B **37**, 785 (1988).

[79] A. J. Sadlej, Collect. Czech. Chem. Commun. **53**, 1995 (1988).

[80] A. J. Sadlej, Theor. Chim. Acta **79**, 123 (1992).

[81] A. J. Sadlej, Theor. Chim. Acta **81**, 339 (1992).

[82] C. Gonzalez and H. B. Schlegel, J. Chem. Phys. **90**, 2154 (1989); J. Phys. Chem. **94**, 5523 (1990).

[83] M. J. Frisch, G. W. Trucks, H. B. Schlegel *et al.*, GAUSSIAN 98, Revision A.7, Gaussian, Inc., Pittsburgh PA, 1998.

[84] See EPAPS Document No. E-JCPSA6-010242 for supporting information on the Cartesian coordinates, total energies and vibrational zero-point energies for selected stationary structures given in Fig. 5. A direct link to this document may be found in the online article's HTML reference section. The document may also be reached via the EPAPS homepage (http://www.aip.org/pubservs/epaps.html) or from ftp.aip.org in the directory/epaps/. See the EPAPS homepage for more information.

[85] Y.-L. Li and D. L. Phillips, Chem. Phys. Lett. **349**, 291 (2001).

[86] A. S. Dneprovskii, D. V. Kuznetsov, E. V. Eliseenkov, B. Fletcher, and J. M. Tanko, J. Org. Chem. **63**, 8860 (1998).

[87] J. E. Chateauneuf, J. Org. Chem. **64**, 1054 (1999).

[88] G. A. Russell, J. Am. Chem. Soc. **79**, 2977 (1957).

[89] G. A. Russell, J. Am. Chem. Soc. **80**, 4987 (1958).

[90] G. A. Russell, J. Am. Chem. Soc. **80**, 4997 (1958).

[91] C. Walling and M. F. Mayahi, J. Am. Chem. Soc. **81**, 1485 (1959).

[92] P. S. Skell, H. N. Baxter III, and C. K. Taylor, J. Am. Chem. Soc. **105**, 120 (1983).

[93] P. S. Skell and H. N. Baxter III, J. Am. Chem. Soc. **107**, 2823 (1985).

[94] N. J. Bunce, K. U. Ingold, J. P. Landers, J. Lusztyk, and J. C. Scaiano, J. Am. Chem. Soc. **107**, 5464 (1985).

[95] P. S. Skell, H. N. Baxter III, J. M. Tanko, and V. Chebolu, J. Am. Chem. Soc. **108**, 6300 (1986).

[96] N. J. Bunce, R. B. Joy, J. P. Landers, and J. S. Nakai, J. Org. Chem. **52**, 1155 (1987).

[97] V. A. Aver'yanov and S. G. Ruban, Kinet. Katal. **27**, 485 (1986).

[98] R. Breslow, M. Brandl, J. Hunger, N. Turro, K. Cassidy, K. Krogh-Jespersen, and J. D. Westbrook, J. Am. Chem. Soc. **109**, 7204 (1987).

[99] C. Walling, J. Org. Chem. **53**, 305 (1988).

[100] K. D. Raner, J. Lusztyk, and K. U. InGold, J. Am. Chem. Soc. **110**, 3519 (1988).

[101] J. M. Tanko and F. E. Anderson III, J. Am. Chem. Soc. **110**, 3525 (1988).

[102] K. D. Raner, J. Lusztyk, and K. U. Ingold, J. Org. Chem. **53**, 5220 (1988).

[103] K. D. Raner, J. Lusztyk, and K. U. Ingold, J. Phys. Chem. **93**, 564 (1989).

[104] K. D. Raner, J. Lusztyk, and K. U. Ingold, J. Am. Chem. Soc. **111**, 3652 (1989).

[105] K. U. Ingold, J. Lusztyk, and K. D. Raner, Acc. Chem. Res. **23**, 219 (1990).

[106] J. E. Chateauneuf, J. Am. Chem. Soc. **115**, 1915 (1993).

[107] D. Wang, Y.-L. Li, W. S. Ho, K. H. Leung, and D. L. Phillips, J. Org. Chem. **67**, 747 (2002).

[108] K.-D. Asmus, Acc. Chem. Res. **12**, 436 (1979).

[109] K.-D. Asmus, D. Bahnemann, C.-H. Fischer, and D. Veltwisch, J. Am. Chem. Soc. **101**, 5322 (1979).

[110] S. A. Chaudhri and K.-D. Asmus, Angew. Chem. Int. Ed. Engl. **20**, 672 (1981).

[111] R. L. Peterson, D. J. Nelson, and M. C. R. Symons, J. Chem. Soc., Perkin Trans. 2 **1978**, 225 (1978).

[112] M. H. Champagne, M. W. Mullins, A. Colson, and M. D. Sevilla, J. Phys. Chem. **95**, 6488 (1991).

[113] L. K. Steffen, R. S. Glass, M. Sabahi, G. S. Wilson, C. Schoneich, S. Mahling, and K.-D. Asmus, J. Am. Chem. Soc. **113**, 2141 (1991).

[114] D. K. Maity, H. Mohan, and J. P. Mittal, J. Chem. Soc., Faraday Trans. **90**, 703 (1994).

[115] M. A. James, M. L. McKee, and A. J. Illies, J. Am. Chem. Soc. **118**, 7836 (1996).

[116] M. D. Sevilla, S. Summerfield, I. Eliezer, J. Rak, and M. C. R. Symons, J. Phys. Chem. **101**, 2910 (1997).

[117] Y. Gaudel, L. J. Marigneir, and J. Belloni, J. Phys. Chem. A **101**, 8979 (1997).

[118] K.-D. Asmus, in *Sulfur-Centered Radicals*, edited by Z. B. Alfassi (Wiley, New York, 1999), p. 141.

[119] Y. Gaudel, H. Gelabert, and F. Guilloud, J. Am. Chem. Soc. **122**, 5082 (2000).

[120] N. C. Baird, J. Chem. Educ. **54**, 291 (1977).

[121] T. Clark, J. Am. Chem. Soc. **110**, 1672 (1988).

[122] P. M. W. Gill, P. Weatherall, and L. Radom, J. Am. Chem. Soc. **111**, 2782 (1989).

[123] A. J. Illies and P. Livant, J. Am. Chem. Soc. **113**, 1510 (1991).

[124] D. K. Maity and H. Mohan, Chem. Phys. Lett. **230**, 351 (1994).

[125] D. K. Maity, H. Mohan, and J. P. Mittal, J. Phys. Chem. **99**, 12195 (1995).

[126] S. P. de Visser, L. J. de Koning, and N. M. M. Nibbering, J. Phys. Chem. **99**, 15444 (1995).

[127] M. L. McKee, A. Nichols, and L. Radom, J. Am. Chem. Soc. **118**, 10571 (1996).

[128] M. Aida, F. Inoue, and M. Kaneko, J. Am. Chem. Soc. **119**, 12274 (1997).

[129] B. Braïda, P. C. Hirberty, and A. Savin, J. Phys. Chem. A **102**, 7872 (1998).

[130] S. P. de Visser, L. J. de Koning, and N. M. M. Nibbering, J. Am. Chem. Soc. **120**, 1517 (1998).

[131] S. Humbel, I. Cote, N. Hoffmann, and J. Bouquant, J. Am. Chem. Soc. **121**, 5507 (1999).

[132] B. Braïda, Lauvergnat, and P. C. Hiberty, J. Chem. Soc. **115**, 90 (2001).

[133] D. K. Maity, J. Phys. Chem. A **106**, 5716 (2002).